How to Cite:
Nalini, M., & Prabavathy, K. (2022). Fruit fly optimization algorithm based modified least squares twin SVM for grading of metacarpophalangeal rheumatoid arthritis. *International Journal of Health Sciences*, *6*(S4), 2743–2760. https://doi.org/10.53730/ijhs.v6nS4.7934

Fruit fly optimization algorithm based modified least squares twin SVM for grading of metacarpophalangeal rheumatoid arthritis

M. Nalini
Research Scholar, Rathinam College of Arts and Science, Coimbatore
*Corresponding author email: Nalini1911@gmail.com

Dr. K. Prabavathy
Assistant Professor, Rathinam College of Arts and Science, Coimbatore
Email: prabavathy.cs@rathinam.in

***Abstract*---**In the past few decades, ultrasound (US) has witnessed a drastic progress in the inflammatory joint diseases field. RA (Rheumatoid arthritis) is possibly the pathology, which has gained the most advantages due to this progress, both with respect to timely diagnosis and monitoring of disease course. Training a professional sonographer is costly and time- constrained whereas some studies pay attention towards automated RA grading techniques and itis possible using machine learning (DL) technique, to yield a highly objective, automated and rapid means of RA diagnosis in clinical environments. Hence, effective MLTs (machine learning techniques) that are less time consuming while achieving better performances in quick recognition of RA diseases should be proposed by combining soft computing methods. With this motivation, this work proposes FFO-MLSTSVM (Fruit Fly Optimization Algorithm Based Modified Least Squares Twin Support Vector Machines) method for Grading of MRA (Metacarpophalangeal RA). This technical work makes use of the parameters and texture characteristics pertaining to ROIs (regions of interest). The focused feature associated with the metacarpophalangeal bone and the dark feature associated with synovial thickening are extracted at the same time using a segmentation technique based on the Modified Fuzzy Auto-Seed Cluster Means Morphological Segmentation, followed by feature extraction using CNNs (convolution neural networks) for ranking the ultrasonic image of MRAs.

***Keywords*---**bone erosion, rheumatoid arthritis, convolution neural networks, medical ultrasound images, fruit fly optimization, modified least squares, twin svm method.

Manuscript submitted: 27 March 2022, Manuscript revised: 9 April 2022, Accepted for publication: 18 May 2022

Introduction

Nearly 0.92% of adult population in India are affected with RA which is a systemic autoimmune disease that makes multiple joints to swell (inflammation). The swelling damages the joints from inside and creates deformities permanently. A considerable number of population depicts continuous discomfit, stiffness, advanced joint degradation, functional incapacity, and advancing morbidity and fatal to life[1]. Disease characterizes itself by a consistent joint inflammation in addition to cartilage and bone destruction with considerably limited movement, reduced quality of life and frequently systemic seriousness. Many advancements have been observed in diagnostic and treatment modalities for RA lately and tertiary care centres in the nation are well within access. Timely diagnosis and rigorous therapy can generally avert disability that can be permanent. Regretfully, this is not the case in many [2].

Detection of the affected finger joint area of RA patients and measuring its seriousness in subsequent phases are vital to diagnose, make decisions on treatment, and for the estimation of the advancement of the disease. In clinical terms, RA criticality is evaluated with the help of the gray-scale-evaluated synovial hyperplasia score, a four-grade semi-quantitative scoring value. Many studies that are relevant to RA severity rating use a dataset made up of x-ray pictures rather than ultrasound images to detect finger joints or identify bone degradations. Physical examination, blood tests, and imaging procedures such as X-ray, MRI, CT, and ultrasound are used to identify clinical symptoms. The technological progress in imaging modalities has stated that MRI is highly responsive in case of RA detection, however its time of capture is high and its process, costly. Ultrasound imaging modality can replace this. Amongst them, Ultrasound imaging is desired as its inexpensive, less dangerous and easily available [3,4]. The gray scale ultrasound imaging helps in evaluating the progress in the disease state by categorizing synovitis and ability to forecast the synovial growth, initial synovitis or an already present one, level of outburst and also giving a sign for the state of anomaly [5]. The change of gray shades in ultrasound image indicates soft tissues, bone and synovial region. RA evaluation can be taken to be an image classification problem.

MLTs in computer science aim to generate predictive data models by using algorithms, methods, and procedures and uncover undefined correlations in data and create tools that exploit definitions, estimations, or suggest conjunctions [6]. DLTs (Deep learning techniques) based on CNNs [7] have recently made significant progress in medical image analysis. DLTs perform substantially better than traditional statistical learning techniques, according to research, resulting in enhanced accuracy and stability. The critical step in these technique involves extracting the differentiating features, which is hard to be introduced from the processed images. The study in [8,9] have performed the localization of the joint area automatically applying histogram and determined osteoarthritis using histogram and SVM. Studies have demonstrated that SVM algorithm perform better than conventional statistical learning techniques, yielding improved accuracy and stability.

With this motivation, in this work, the texture features associated with the synovium ultrasonic image are used for classifying the MRAs ultrasonic images employing FFO-MLSTSVM algorithms. The geometric information relevant to synovium thickening and image details associated with bone injuries have been rarely used in the studied literature. The geometric and texture properties of synovium thickening and bone degradation are detected and predicted using a ranking technique of MRAs in ultrasonic images in this study. The work's key contribution is as follows:

- An entire RA image sample are taken as input
- Segmentations are dependent on image extracts of metacarpophalangeal bone's focused features and dim features of synovial thickening in parallel using Modified Fuzzy Auto-Seed Cluster Means Morphological Segmentation method.
- Feature extractions using CNNs .
- Classifications using FFO-MLSTSVM method where the set of parameters in MLSTSVM is tackled efficiently by the FFO technique.

The research work is structured as given: In section 2, the literature works related to the current work is presented. Section 3 studies the proposed methodology and dataset. In section 4, the results of the experiments are presented and discussed. At the end, Section 5 provides the conclusion of the work with future work.

Related Work

The study in [10] described the algorithms proposed for the segmentation of 1) the 3-D bone surface and 2) the 3-D joint capsule area. The earlier 2-D bone extraction techniques are modified and extended to 3-D and the robustness of the algorithm towards the loss in intensity owing to surface normals projected away from the inward acoustic beams is improved. The acquired bone surfaces, which are integrated with a joint-oriented anatomical framework are considered for initializing a rough localization on the joint capsule area. The joint capsule segmentation process is fine tuned in an iterative manner by using a probabilistic speckle model. The objective of this work was to check BMDs (bone mineral densities), TBSs (trabecular bone scores) along with their fusion to detect RA patients suffering with VFs (vertebral fractures) [11].

The objective of this work in [12] was about assessing the novel automated BoneXpert technique compared to the actual form of DXR in RA patients. The comparison highlighted on the acceptance of their measurements used for predicting Metacarpal Index (MCI)and with respect to the RA criticality like the Larsen Score predicts. Moreover, the capability of Bone Health Index (BHI)in quantifying the periarticular bone loss was assessed. The study in [13] proposed an innovative quantitative technique to automatically detect bone damages on hand radiographs in order to assist radiologists Initially, the suggested strategy used a hand radiograph to perform rough segmentation of phalanges regions, and then used MSGVFs (multi-scale gradient vector flows) Snakes method to extract elaborate phalanges regions. Finally, using a deep CNN classifier, selected ROIs were recognised in terms of the presence or absence of bone damages.

The study in [14], utilized simple hand radiographs and attempted developing an automatic diagnostic technique that uses the CNNs so that physicians will find it easy during the diagnosis of RA. CNNs are DLTs based on the design of multi-layer neural networks. The study [15] revealed that deep CNNs may be used to rank X-ray pictures of patients with RA in a completely autonomous, rapid, and repeatable manner. The study in [16] reviewed and provided a short outline on the pathophysiology of RA and its relationship to carotid atherosclerosis as imaged with B-mode ultrasonography Lacunas with traditional risk scores explained, as well as the role performed by MLTs in tissue characterization algorithms, which could aid in the assessment of cardiovascular risk in RA patients. The objective of the work introduced in [17] helped in the classification and categorization of hand arthritis levels for patients, who may be on the way of or advanced hand arthritis, employing MLTs. Stage classifications were performed with the help of finger border detections, progressive curvature analysis, PCAs (principal components analyses), SVMs (support vector machines) and KNNs (K-nearest neighbours).

A grading technique for the detection and estimation of the geometric and textural aspects of synovium thickening and bone injury was provided in [18]. SVMs and various feature descriptors, including as GLCMs, LBPs (local binary patterns), and GLCMs + LBPs, were utilised to grade the ultrasonic image of MRAs in order to harness the desirable capability of classifications. Even though the accuracy rate achieved with SVM is high, in scenarios where the number of features for every feature is more than the number of training data samples, the performance of SVMs will be poor. So an effective machine learning method for a fast recognition of RA diseases should be proposed that should be less time consuming and should achieve better performance by combining soft computing methods.

Proposed Methodology

The proposed approach uses phases depicted as fig.1. Initially, all ROI samples of three groups of MRAs in ultrasound pictures were used along with healthy metacarpophalangeal joint images. Quantitative feature metrics and textural were obtained from the ROI image of RA ultrasound pictures in this phase to define various types of RA in ultrasound images. Using segmentations based on the Modified Fuzzy Auto-Seed Cluster Means Morphological method, highlighted features of metacarpophalangeal bones and the dim features of synovial thickening were extracted simultaneously and their feature vectors generated using CNNs. To leverage the desirable capability of classifications, this work applied FFO-MLSTSVMs for ranking ultrasonic images with MRAs.

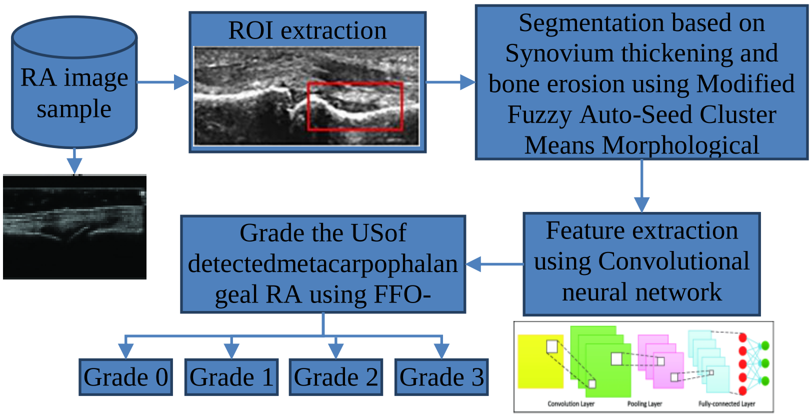

Fig 1. Architecture Diagram of proposed FFO-MLSTSVM based grading method of RA ultrasonic images

Input RA US Image Sample

The First Teaching Hospital of Tianjin University of Traditional Chinese Medicine provided complete RA imaging samples. In clinical medicine, MRAs are one of four main categories based on synovium thickening [18]. The synovium does not thicken in grade 0. Grade 1 synovial thickening is very light, with the thickening site running via the connecting line between the upper areas of two articular bones. Grade 2 synovial thickening occurs when the thickening region of the synovium spreads along the top section of the articular bones. Synovial thickening is severe in Grade 3, and the thickening area spreads from the triangular region encircling the joint to the centre and end of the bone scale. Furthermore, MRAs were graded according to the degree of bone injury. In an ultrasonic image corresponding to bone deterioration, the flaw of an illuminated line of bone cortex can be seen in the long axis as well as the short axis. Grade 0 indicates that there has been no bone deterioration. The bone cortex in Grade 1 has a rough surface and is defect-free. In Grade 2, there appears to be a problem with the bone cortex. In Grade 3, there is a large deficiency in the bone cortex. In ultrasound pictures, Figure 2 depicts the symptoms of bone damage [18].

ROI Extraction

ROI samples were created from three groups of MRA ultrasound pictures and a healthy metacarpophalangeal joint image in this study. ROIs had three different sizes, depicted in red, cyan, and green rectangular boxes that could be cut in the area of synovial thickening images or bone degeneration image [18].

Modified Fuzzy Auto-seed cluster means morphological (MFACMM) segmentation

Segmentations are executed using fuzzy concept, which plays an essential role in data categorizations. The fuzzy membership function calculates degree of proximity between pixels and reference clusters' centre values. These fuzzed data assist in segmenting a given image into a number of regions by retaining their spatial positions (clusters). The soft membership function used in this study simplifies the segmentation process as hard threshold based segmentations make it difficult to easily partition images RO|Is. In ultrasonic pictures, synovium thickening and bone degeneration are normally black, whereas metacarpophalangeal bones are lighter in color. Based on MFACMM [19], this work provides a technique for extracting the characteristics of metacarpophalangeal bone and synovial thickening in parallel. The algorithm used to determine initial cluster reference values independently have been designed in this work as it allows this segmentation process to be totally automated. Two measurements can be obtained using this technique: synovium thickness and the area on synovium thickening and metacarpophalangeal bone. The following are the stages of MFACMM Segmentations and detailed below: Step 1: At first, the ROI $I\,(x, y)$ which consists of synovial thickening areaand bone erosion area, was first obtained which was segmented into two regions: synoviumthickening and metacarpophalangeal bone. To this end, two initial cluster values must be selected. To fully automate this segmentation, these two initial clusters $c$were computed separately using the following

$$c_1 = \frac{\Sigma(\sum_{i=1}^{m} \max(I(i,:)))}{N} \text{ and } c_2 = \frac{\Sigma\left(\sum_{j=1}^{m} \max(I(i,:))\right)}{N} \quad (1)$$

Where $m$refers to the number of rows, $n$indicates the number columns in RA of US image $I(i, j)$and N signifies the overall number of non-zero pixels.
Step 2: The difference between each pixel and clusters were calculated , and two distance matrixes $Dist_1$and $Dist_2$were created for both c_1 and $c_2$correspondingly with the expressions below:

$$Dist_1 = [c_1 - I(i, j)]^2 \text{ and } Dist_2 = [c_2 - I(i, j)]^2 \quad (2)$$

Where $i = 1,2, \dots, m$ and $j = 1,2, \dots, n$.
Step 3: The distance matrix $Dist_1$ and $Dist_2$acquired in the earlier step undergoes smooth fuzzification applying the below expressions, and later the coefficients get normalized and fuzzified uinsg a real parameter $r > 1$such that their sum is 1 and theultimate smooth fuzzified data was saved in $Fuzzy_1$ and $Fuzzy_2$.

$$Fuzzy_1 = \frac{1}{(Dist_1)^{\frac{2}{r-1}}} \text{ and } Fuzzy_2 = \frac{1}{(Dist_2)^{\frac{2}{r-1}}} \quad (3)$$

In the case of $r$equivalent to 2, this is same as linearly normalizing the coefficient to render their sum 1.
Step 4: Fuzzy rule based assignment was performed on an image $Fuzzy(i, j)$ with regard to $Fuzzy_1$ and $Fuzzy_2$ and the segmented image seg_1 and seg_2 are computed as follows:

$$seg_1(i, j) = I(i, j), if Fuzzy_2(i, j) < Fuzzy_1(i, j) \text{and}$$
$$seg_2(i, j) = I(i, j), if Fuzzy_2(i, j) > Fuzzy_1(i, j) \quad (4)$$

Where seg_1refers to the segmented image with regard to the first cluster c_1 and seg_2 is one more segmented image with regard to cluster c_2.
Step 5: The segmented regions seg_1 and seg_2were fine tuned by updating the cluster valuec_1 and $c_2$applying the expressions below.

$$c_{1_{new}} = \frac{\sum(seg_1(i,j)\neq 0)}{N_1} \text{ and } c_{2_{new}} = \frac{\sum(seg_2(i,j)\neq 0)}{N_2} \quad (5)$$

Where N_1 and N_2refers to the overall number of non-zero pixels in seg_1 and seg_2correspondingly.
Step 6: Step 1 to 5 were performed once more using the new cluster centre value $c_{1_{new}}$ and $c_{2_{new}}$. The iteration of this process was continued till the difference between two subsequent $c_{1_{new}}$ and $c_{2_{new}}$become the least values.
Step 7: The binary images are generated using mathematical morphology. Synovium thickening and metacarpophalangeal erosion zones are refined in processed binary images. Finally, the thickness of the synovium, the amount of synovial thickening, and the metacarpophalangeal area are computed.

Feature extraction using CNN

This section studies the extraction of three feature aspects, which include the region of bone degradation and synovial thickening (F1), synovial thickness (F2), and the shape taken by the synovial thickening region (F3). DLTs or much precisely CNNs are used in the modified form of artificial neural networks. The benefit achieved using DLTs involves the capability of the networks to learn for extraction of features during training. They extract features independently utilizing convolution kernels. In addition, the convolution layers have a group of small parameterized filters. They are commonly referred to as kernels or convolution filters, and they are employed in each layer to generate a tensor of feature maps, as shown in Fig. 2.

In this technique, the processing of the ultrasound images are performed and synovial regions of various ranks undergo segmentation applying the contour method. These segmented images are sent to the layered CNN to analyze the various ranks of the synovial region. CNNs are used forshowing the grading given to the synovial area in accordance with the intent of analysis and diagnosis of the arthritiscondition. The CNN evaluates the input set of images functioning as the layers using which a part of the regionis obtained for classification. These samples undergo convolution in the convolution layers where there the subsamples undergo maximum pooling from the input images. Therefore, these networks are entirely tied up to specify the output layer. The framework of the CNN network having the input segmented images made up of 227 × 227 pixels is shown as the below steps:

- Conv1 (convolution filters of size 3 × 3, stride of 1, padding of 1, and kernels of 32) are used. Conv1 = 227 − 3 + (2 × 1) 1 + 1 = 227 In the case of the square feature maps, 227 × 227 × 32 = 1648928 neurons are present in the feature map of the first convolution layer.
- MaxPooling1 is equivalent to the ratio of the earlier image size and the stride number: Max Pooling1 = 227 2 ≈ 113 In the case of the square feature maps, 113×113×32 = 408608 neurons exist in the feature map of the first max pooling layer.
- Conv2 (convolution filters of size 5 × 5, stride of 1, padding of 2 and kernels of 64) are used. Conv2 = 113 − 5 + (2 × 2) 1 + 1 = 113 For the square feature

maps, 113 × 113 × 64 = 817216 neurons exist in the feature map of the second convolution layer.

- MaxPooling2 is decided in the same method that is applied in MaxPooling2: Max Pooling2 = 113 2 ≈ 56 For the square feature maps, 56 × 56 × 64 neurons exist in the feature map of the second max pooling layer.
- Conv3 (convolution filters of 7×7 used with stride of 1, padding of 3 and kernels of 128). Conv3 = 56 − 7 + (2 × 3) 1 + 1 = 56 For the square feature maps, 56 × 56 × 128neurons are present in the feature map of the third convolution.
- The class scores are computed by the fully-connected (FC) layer, which results in a volume of size 112. All of the features learned by the previous levels are combined in this layer. The number of classes in the data set equals the size of FC's output. The FC input size is set to 401408 in this work, and the output size is set to 2.

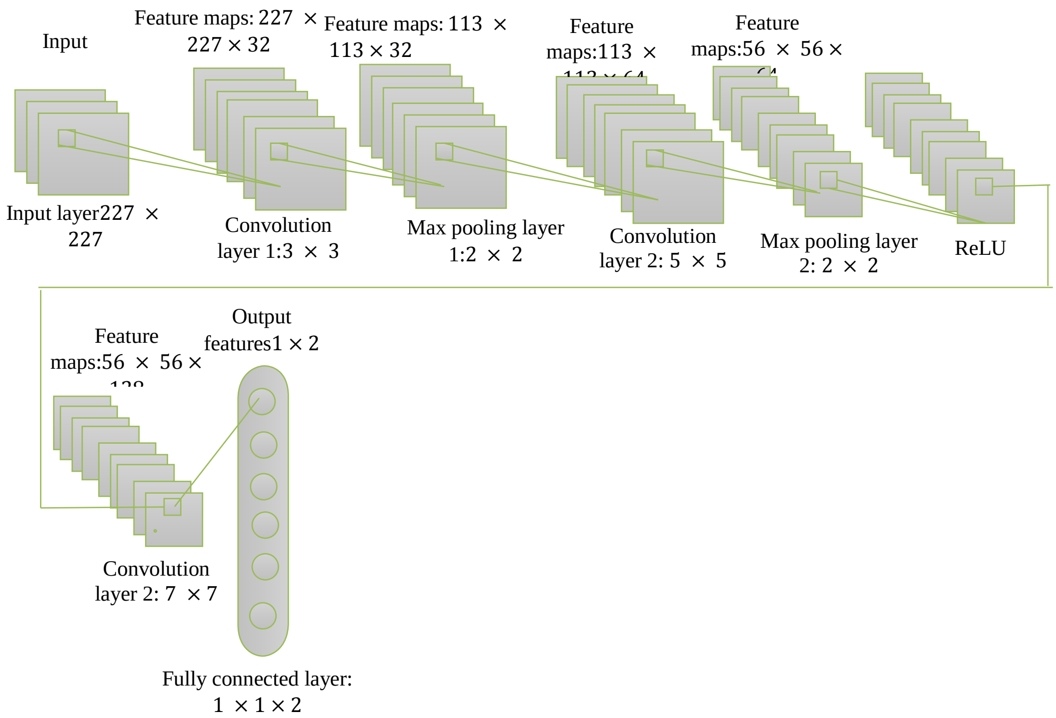

Fig 2.CNN based feature extraction process diagram

Proposed FFO-MLSTSVM

MLSTSVM contains four parameters c_1, c_2, sigma1 and sigma2 that must be initialized by the user where c_1 and $c_2$indicates the amount of error for every class and sigma1 and sigma2 quantifies the effect of error has on every hyperplane. These four parameters have a huge dependence on thenature of the problem implying that for various problems, their optimum values would be different. Due to this, the accuracy of MLSTSVM is affected and is regarded to be a setback. In this work, the FFO algorithm is utilized to get the best global values for MLSTSVM parameters. Initial classification tests were performed on healthy and afflicted images of the metacarpophalangeal joints. Grade 0 ultrasound images served as positive samples, while Grade 1, Grade 2, and Grade 3 ultrasound images served as negative samples. The classifier used was MLSTSVM.

MLSTSVM

In this approach, consider k-Class scenario, MLSTSVM classifier helps resolve the K-linear equations and then K hyper-planes that are non-parallel are generated, with one hyper-plane assigned for every class. It builds k-binary LSTSVM classifiers and ith LSTSVM classifier takes the features of ith class having positive class names and features of remaining classes having negative class labels. Assume the features of ith category are given by the matrix $X_i \in R^{f_i \times n}$, where $f_i$represents the number of features in ith class. The features of the remaining classes are specified by the matrix $Y_i \in R^{(f-f_i)\times n}$ as:

$$Y_i = [(X_1)^T, \dots, (X_{i-1})^T, (X_{i+1})^T, \dots, (X_k)^T]^T \qquad (6)$$

Here, consider the linear model with4-class classification problem and the features of every class are represented using diverse shapes for exact visualization of the classes. MLSTSVM classifier chooses three hyper-planes, one for every class to be plane 1, plane 2, plane 3 and plane 4 for class 1, class 2, class 3and class 3 correspondingly. Hyperplanes are acquired such that the features of every class stay very near to its correspondingly hyperplane and be clearly separated from other hyperplanes and$i$th hyper-plane as per the decision function $d$given as:

$$df_i = (w_i \cdot x) + b_i = 0 \qquad (7)$$

Where $w_i \in R^n$indicates the normal vector to the hyper-plane, $b_i \in R$stands for the bias value. The objective function of ith linear MLSTSVM classifier is defined as:

$$\min(w_i, b_i \xi_i) \frac{1}{2} \|X_i w_i + v_{i1} b_i\|^2 + \frac{c_i}{2} \xi_i^T \xi_i$$
$$s.t. (Y_i w_i + v_{i2} b_i) + \xi_i = v_{i2} \qquad (8)$$

Where $c_i$denotes penalty parameter, $v_{i1} \in R^{f_i}$ and $v_{i2} \in R^{f-f_i}$ are two vectors of 1's and $\xi_i$is the slack variable. The first term in the objective function provides the measure of the squared sum distances of the features of ith class. Minimizing it maintains the hyper-plane very close with the ith class. The second term of the objective function helps reduce the misclassification error owing to the features belonging to other classes. Therefore, in this manner, the hyper-plane is in the close proximity of the features of ith class and at a maximum distance possible from the features belonging to the rest of the classes. Lagrangian function of objective function is computed as:

$$L(w_i, b_i, \xi_i, \sigma_i) = \frac{1}{2} \qquad (9)$$

Adopting Karush–Kuhn–Tucker (KKT) criterion are acquired by performing a differentiation on the above equation with respect to $w_i, b_i, \xi_i$and σ_i as:

$$\frac{\partial L}{\partial w_i} = X_i^T(X_i w_i + v_{i1} b_i) - Y_i^T \sigma_i = 0 \tag{10}$$
$$\frac{\partial L}{\partial b_i} = v_{i1}^T(X_i w_i + v_{i1} b_i) - v_{i2}^T \sigma_i = 0 \tag{11}$$
$$\frac{\partial L}{\partial \xi_i} = c_i \xi_i - \sigma_i = 0 \tag{12}$$
$$\frac{\partial L}{\partial \sigma_i} = (Y_i w_i + v_{i2} b_i) + \xi_i - v_{i2} = 0 \tag{13}$$

Eqs. (10) and (11) lead to:

$$\begin{bmatrix} X_i^T \\ v_{i1}^T \end{bmatrix} [X_i \quad v_{i1}] \begin{bmatrix} w_i \\ b_i \end{bmatrix} - \begin{bmatrix} Y_i^T \\ v_{i2}^T \end{bmatrix} \sigma_i = 0 \tag{14}$$

Here define the $A_1 = [X_i \quad v_{i1}]$ and $A_2 = [Y_i \quad v_{i2}]$ and $u_i = \begin{bmatrix} w_i \\ b_i \end{bmatrix}$. using these notations, Eq. (14) may be written again as:

$$A_1^T A_1 u_i - A_2^T \sigma_i = 0 \tag{15}$$
$$u_i = (A_1^T A_1)^{-1} A_2^T \sigma_i \tag{16}$$

Lagrangian parameter is obtained fromEq. (12) and Eq. (13)

$$\sigma_i = c_i(v_{i2} - A_2 u_i) \tag{17}$$

Eqs. (14) and (16) lead to:

$$\begin{bmatrix} w_i \\ b_i \end{bmatrix} = u_i = \left(A_2^T A_2 + \frac{1}{c_i} A_1^T A_1\right)^{-1} A_2^T v_{i2} \tag{18}$$

Eq. (18) decides the hyper-plane for ith class. So, hyper-plane is obtained for every class. This classifier helps in the prediction of the class $k = 4$for a test feature 'x' based on its distance from every hyper-plane. The class, with respect to the hyper-plane that stay close to 'x', is designated to it. The decision functiondf of MLSTSVM classifier is expressed as follows:

$$df(x) = \arg \min_{i=1,..,k} \frac{|w_i \cdot x + b_i + \sigma_i|}{w_i} \tag{19}$$

FFA- MLSTSVM

The primary concept of FFA- MLSTSVM is to get the ideal parameters of twin SVMs using FFA. The parameters are shown by the fruit fly's position coordinates. A scent concentration judgement function is present in each fruit fly. Classification accuracy is calculated as a fitness function in FFA-MLSTSVM. The coordinates of flies are considered candidate parameters of MLSTSVM. The distance between the hyperplane and the samples in class -1 is clearly affected by the parameter c i. In general, the lower the value of c_i, the less the distance will be highlighted and the shorter the distance will be. As a result, the c_i cannot be too small, or the hyperplane for class +1 will be too close to the samples in class -1, reducing the classification accuracy significantly. Using (8)'s object function, it is discovered that c_1 must be very large, or the framework will ignore the distance between the samples and their hyperplane, resulting in poor classification results. The parameter $c_2$and the remaining parameters affect the classification accuracy similarly.

Therefore, all the parameters must not be very big or too less and it is only necessary to find the most appropriate parameter in a restricted level. But, the association is possibly not a plain mapping correlation, which is, there are various extreme points resulting in the difficulty level to increase. The analysis above has shown that the parameter selection problem concerned with MLSTSVM s depicts two characteristics. The first one indicates that the highly appropriate parameters could be got through just searching within a restricted range. Another one involves multiple extreme. FFA is skilled with respect to the type of problems having the two characteristics. First, FFA initializes the fragrance using a set of random numbers within a restricted range and chooses the most appropriate parameters of MLSTSVM from the random numbers based on the classification accuracy achieved with MLSTSVM and the parameters are recorded. Later the random numbers will be modified towards the most desirable parameters and the modified number along with one more set of random numbers will be considered to be the new candidates of the highly desirable parameters.

FFA proceeds to choose the highly appropriate parameters of MLSTSVM to create the new candidates based on the classification accuracy achieved with MLSTSVM. In case there are no better parameters, FFA saves the parameters, the candidate parameters are adjusted towards the more favourable parameters and the modified number along with a new set of random numbers is considered to be the new candidate parameters. Otherwise, FFA will just include a new set of random numbers for the primal random numbers and not the adjusted ones and proceeds. As seen from the descriptionabove, it is not hard to see that FFA pushes the initial random parameters to get along a route towards the highly appropriate parameter instead of choosing in random. FFA-MLSTSVM later gets the optimal parameters required, and later the optimal parameters can be used to decide the twin SVM model. Toboost the global search capability, some fruit flies always fly in random so that FFA can avoid the local optima. The steps of FFA-MLSTSVM is given below:

- Step 1: Set the MLSTSVM parameters c_1, c_2, and sigma, as well as the swarm position range, iteration number N, and group size S to their default values. Randomize the position of the fruit fly swarm.
- Step 2: Apply osphresis to three-quarters of the fruit flies seeking food and randomise the direction and distance. $If\ i < \left(\frac{1}{3}\right) S$then $X_i = X_{axis} + Rand\ Y_i = Y_{axis} + Rand$
- $Else\ The\ rest\ fly\ randomly\ X_i = Rand, Y_i = Rand$, where random value is denoted as $Rand$.
- Step 3: Because the location of the food is unknown, the distance to the origin is estimated first (dist), followed by the SC (smell concentration) judged value which gives the reciprocal of distance.

$$dist_i = \sqrt{X_i^2 + Y_i^2}; SC_i = \frac{1}{dist_i}, i = 1,2, \dots . N$$

- Step 4:Use SC in the smell concentration judgment function so that the smell concentration ($Smellconce_i$) of every location of the fruit fly is found.
- $Smellconce_i = Function(SC_i)$
- Step 5:Get the fruit fly with maximum smell concentration amongst fly swarm fruits. $[bestSmell\ bestIndex] = \max(Smell)$
- Step 6: Maintain the best smell concentration value and x, y coordinate, and the fruit fly swarm will use its sight to fly towards that location throughout this time..
- $Smellbest = bestSmell$
- $X\_axis = X(bestIndex)$
- $Y\_axis = Y(bestIndex)$
- Step 8:Decide if the maximal number of iterations is attained. If achieved, the iteration is stopped. Else, increment the number of iteration by one, and repeat Step 2–5 and check whether the smell concentration is much better than the earlier iterative smell concentration, and if true, move to Step 6.
- Step 9:During every iteration, a neighbor will be chosen in random. In case the chosen neighbor exhibits improved accuracy compared to the present state, the chosen neighbor will be considered and its parameters values (c and sigma) utilized as new parameter values and at last, the final best smell concentration value is found and x, y coordinate, the coordinates constitute the values of the optimum parameters that have to be found. Then use them into MLSTSVM and move to next step.
- Step 10:Training Phaseof MLSTSVM and define two matricesA_1 and A_2also choose the penalty parameter $c_i > 0$ Solve Equations. (10)–(13) and assess hyper-plane parameters as per Eq. (18).
- Step 11:Testing Phase of MLSTSVM, where the class is designated to new data point applying the decision function as seen in Equation.(19) and the perpendicular distances are measured from every hyper-plane.
- Step 12:Determine class by applying (19) i.e., the class is allocated to pattern based on which the respective plane is close.
- Step 13: Stop the operation. Using this flow chart, the process of the proposed FFA- MLSTSVM algorithm is intuitively understood as shown in Fig.3.

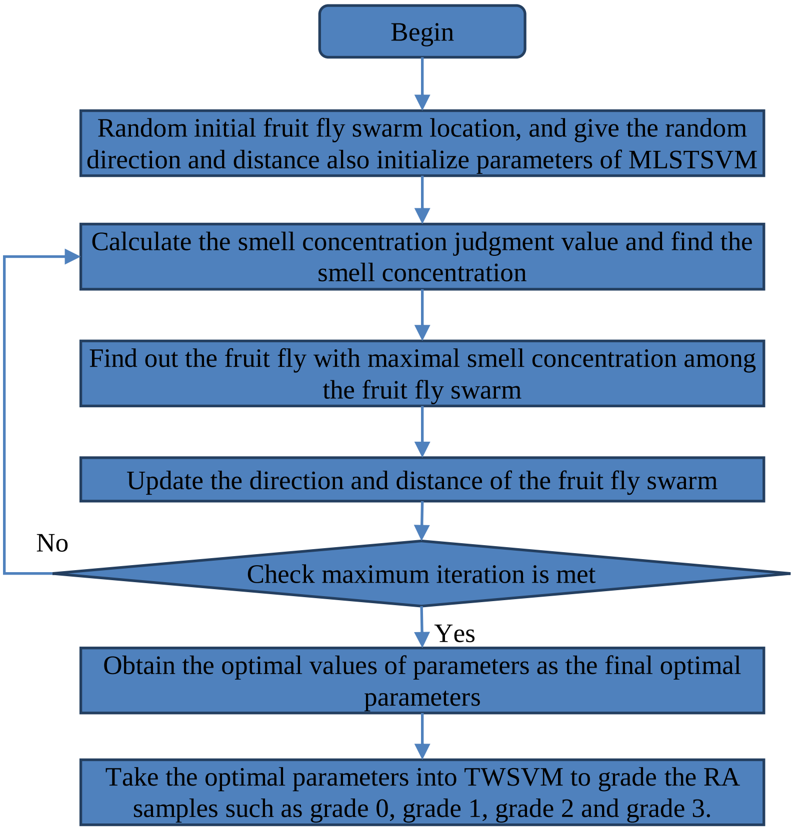

Fig 3. Flowchart of FFA-MLSTSVM

Experimental results and discussion

To quantitatively evaluate the performance achieved with the proposed FFA-MLSTSVM grading model and compared with existing model SVM [18] and CNN [21] computed four popular machine-learning assessment metrics, which include accuracy, precision, recall, and F1measure. The calculation of these metrics could be done using the prediction outcomes of each one of the verified images. Using the binary classification problem of healthy individuals and the patients affected with bone erosion and synovial thickening (Grade 0 vs.Grade 1/2/3) for US samples,

$$accuracy = \frac{TP + TN}{TP + FP + FN + TN} \times 100\%$$

$$precision = \frac{TP}{TP + FP} \times 100\%$$

$$recall = \frac{TP}{TP + FN} \times 100\%$$

$$F1measure = \frac{2 \times percision \times recall}{precision + recall}$$

Precision Result comparison

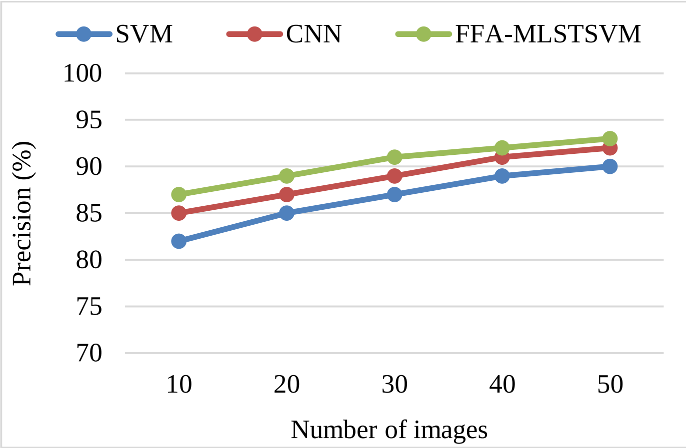

Figure 3.3.2. Precision performance comparison

Figure 3.32 illustrates theresults of precision comparison carried out between SVM, CNN and FFA-MLSTSVM. It can be observed from the figure that the FFA-MLSTSVM technique can yield an increase in precision rate in comparison with other techniques. It is an efficient means of obtaining the cluster center exactly achieving the maximum precision rate of 93%. On the precisioncomparison between the available SVM and CNN providing low precision rates than the FFA-MLSTSVM, FFAare able to improve the generalization capability of MLSTSVM to improve classification precision.

F-measure Result Comparison

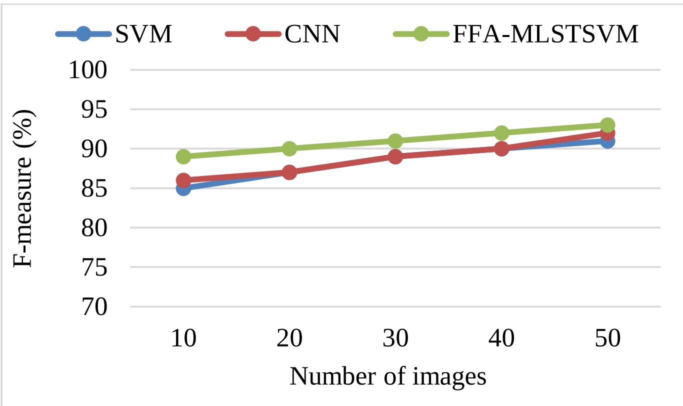

Figure 3.32. F-measure performance comparison

Figure 3.32 illustrates the results obtained from the comparison in terms of F-measure between proposed SVM, CNN and FFA-MLSTSVM. The proposed FFA-MLSTSVM technique yields an improved value of F-measure 93%. In comparison with the F-measure rate with the available method SVM and CNN are providing fewer rates, which shows the proposed work can yield improved grading outcomes for RA. The stability and improved f-measure of FFA-MLSTSVMyields a feasible solution for a classification problem of semi-quantitative condition such as this and also compromise for the inconsistency of diagnosis that clinicians have made.

Recall Result Comparison

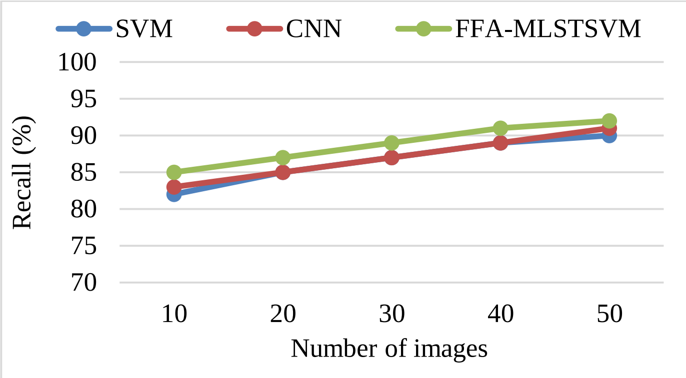

Figure 6.4. performance comparison in terms of recall

Figure 6.4 illustrates the recall comparison results between proposed SVM, CNN and FFA-MLSTSVM. The proposed FFA-MLSTSVM technique yields an improved 92%recall value. Using the results, it is well knowing that proposed FFA-MLSTSVM yields a better recall rate value implying the superior cluster formation rate. When comparing the recall rate among the available techniques SVM and CNN yields low recall rate, which reveals that the proposed work can yield improved grading results compared to the available method. Most critically, the combination of segmentation and CNN based feature extraction used in this work mitigated the issue of the deficit of large, correctly identifying bone erosion and synovial thickening, a problem often seen in clinical RA image analysis. From this, the potential application utility of the proposed CNN-based RA grading technique in being of help to specialized clinicians during diagnosis is confirmed.

Accuracy comparison

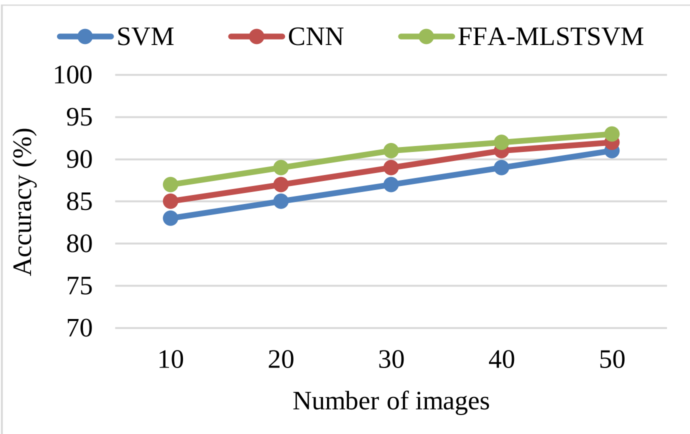

Figure 6.5. Result of Accuracy

From the above Figure 6.5, the graph explains that the accuracy comparison for prediction of cluster centre. When number of data increased according with the accuracy value is increased linearly. From this graph, it is learnt that the proposed FFA-MLSTSVM effectively select the cluster centre with high accuracy of 93% for cluster centre selection. However, the previous methods such as SVM and CNN attains low accuracy than the FFA-MLSTSVMin terms of better classification results for RA with high accuracy rate. The main FFA strategy for MLSTSVM training is the usage of a pre-trained network with optimal parameters and used CNN in the form of a feature extractor and then refining the pretrained network on the target medical image data and thus improves the accuracy value.

Conclusion and Future work

Quantification of RA criticality has always remained a hard problem in diagnosisowing to its semi-quantitative score condition. In accordance with the FFA-MLSTSVM algorithm, an automated classification technique of RA ultrasound images is proposed. Firstly, performed the auto-localization of the synovium lesion region along the bone erosion using the MFACMM. Highlighting on image feature extraction depending on CNNs, the fundamental CNN model is constructed.FFA-MLSTSVM were used for the classification of four gradings for RA ultrasonic images. The overall accuracy achieved with the four gradings classification is close to 93%, whereas the overall accuracy attained with two-grading classification is nearly 95%. It is shown from the results that the proposed technique yield outstanding performances that can be compared with RA specialists in multi-class classification. The potential outcomes achieved with the proposed FFA-MLSTSVM-based RA grading technique is capable of providing a goal and exact reference to help in RA diagnosis and training the sonographers. In the future, more focusing is needed in deep learning based classification over MRAs ultrasonic images.

References

1. Van Der Velde G, Pham B, MacHado M, Ieraci L, Witteman W, et al. Cost-effectiveness of biologic response modifiers compared to disease-modifying antirheumatic drugs for rheumatoid arthritis: A systematic review. Arthritis Care Res. 2011; 63:65–78.
2. Calabresi E, Petrelli F, Bonifacio AF, Puxeddu I, Alunno A. One year in review 2018: pathogenesis of rheumatoid arthritis. ClinExpRheumatol. 2018;36:175-84.
3. Martins N, Sultan MS, Veiga D, Ferreira M, Coimbra M. Joint capsule segmentation in ultrasound images of the metacarpophalangeal joint using a split and merge approach. InBiomedical& Health Informatics (BHI), 2018 IEEE EMBS International Conference on 2018 Mar 4 (pp. 243-246). IEEE.
4. Hemalatha RJ, Vijayabaskar V. Medical image segmentation algorithm for ultrasound images, biomedicine. International Journal of Biomedical Sciences. 2017;37(01):002-007.
5. Brown AK, Quinn MA, Karim Z, Conaghan PG, Peterfy CG, Hensor E, et al. Presence of significant synovitis in rheumatoid arthritis patients with disease-modifying antirheumatic drug–induced clinical remission: evidence

from an imaging study may explain structural progression. Arthritis & Rheumatology. 2006;54(12):3761-73.

6. Kim, K.J.; Tagkopoulos, I. Application of machine learning in rheumatic disease research. *Korean J. Intern. Med.* 2019, *34*, 708–722.
7. LeCun, Y., Bengio, Y., & Hinton, G. (2015). Deep learning. *nature*, *521*(7553), 436-444.
8. Tiulpin A, Thevenot J, Rahtu E, Saarakkala S. A novel method for automatic localization of joint area on knee plain radiographs. InScandinavian Conference on Image Analysis. SCIA.2017:290-301.
9. Gornale SS, Patravali PU, Marathe KS, Hiremath PS. Determination of osteoarthritis using histogram of oriented gradients and multiclass SVM. International Journal of Image, Graphics & Signal Processing. 2017;9(12).
10. Cao, K., Mills, D. M., Thiele, R. G., &Patwardhan, K. A. (2015). Toward quantitative assessment of rheumatoid arthritis using volumetric ultrasound. *IEEE Transactions on Biomedical Engineering*, *63*(2), 449-458.
11. Bréban, S., Briot, K., Kolta, S., Paternotte, S., Ghazi, M., Fechtenbaum, J., & Roux, C. (2012). Identification of rheumatoid arthritis patients with vertebral fractures using bone mineral density and trabecular bone score. *Journal of Clinical Densitometry*, *15*(3), 260-266.
12. Pfeil, A., Thodberg, H. H., Renz, D. M., Reinhardt, L., Oelzner, P., Wolf, G., &Böttcher, J. (2017). Metacarpal bone loss in patients with rheumatoid arthritis estimated by a new Digital X-ray Radiogrammetry method–initial results. *BMC musculoskeletal disorders*, *18*(1), 1-10.
13. Murakami, S., Hatano, K., Tan, J., Kim, H., & Aoki, T. (2018). Automatic identification of bone erosions in rheumatoid arthritis from hand radiographs based on deep convolutional neural network. *Multimedia Tools and Applications*, *77*(9), 10921-10937.
14. Üreten, K., Erbay, H., &Maraş, H. H. (2020). Detection of rheumatoid arthritis from hand radiographs using a convolutional neural network. *Clinical rheumatology*, *39*(4), 969-974.
15. Rohrbach, J., Reinhard, T., Sick, B., &Dürr, O. (2019). Bone erosion scoring for rheumatoid arthritis with deep convolutional neural networks. *Computers & Electrical Engineering*, *78*, 472-481.
16. Khanna, N. N., Jamthikar, A. D., Gupta, D., Piga, M., Saba, L., Carcassi, C., ... & Suri, J. S. (2019). Rheumatoid arthritis: atherosclerosis imaging and cardiovascular risk assessment using machine and deep learning–based tissue characterization. *Current atherosclerosis reports*, *21*(2), 7.
17. Akhbardeh, F., Vasefi, F., MacKinnon, N., Amini, M., Akhbardeh, A., &Tavakolian, K. (2019, July). Classification and Assessment of Hand Arthritis Stage using Support Vector Machine. In *2019 41st Annual International Conference of the IEEE Engineering in Medicine and Biology Society (EMBC)* (pp. 4080-4083). IEEE.
18. Yang, T., Zhu, H., Gao, X., Zhang, Y., Hui, Y., & Wang, F. (2020). Grading of Metacarpophalangeal Rheumatoid Arthritis on Ultrasound Images Using Machine Learning Algorithms. *IEEE Access*, *8*, 67137-67146.
19. Manikandan, T., &Bharathi, N. (2016). Lung cancer detection using modified Fuzzy Auto-seed cluster means morphological segmentation and SVM classifier. *Journal of medical systems*, *40*(7), 1-9.

20. Wiatowski, T., &Bölcskei, H. (2017). A mathematical theory of deep convolutional neural networks for feature extraction. *IEEE Transactions on Information Theory*, *64*(3), 1845-1866.
21. J. Tang, Z. Jin, X. Zhou, W. Zhang, M. Wu, Q. Shen, et al., "Enhancing convolutional neural network scheme for rheumatoid arthritis grading with limited clinical data", *Chin. Phys. B*, vol. 28, no. 3, Mar. 2019.